

Solving the kilo-second QPO problem of the intermediate polar GK Persei

L. Morales-Rueda¹, M. D. Still² and P. Roche¹

¹*Astronomy Centre, University of Sussex, Falmer, Brighton BN1 9QJ (lmorales@star.cpes.susx.ac.uk, pdr@star.cpes.susx.ac.uk)*

²*Physics and Astronomy, University of St. Andrews, North Haugh, St. Andrews, Fife KY16 9SS (mds1@st-and.ac.uk)*

Accepted 1999 January 20. Received 1998 December 16; in original form 1998 July 29.

ABSTRACT

We detect the likely optical counterpart to previously reported X-ray QPOs in spectrophotometry of the intermediate polar GK Per during the 1996 dwarf nova outburst. The characteristic timescales range between 4000–6000s. Although the QPOs are an order of magnitude longer than those detected in the other dwarf novae we show that a new QPO model is not required to explain the long timescale observed. We demonstrate that the observations are consistent with oscillations being the result of normal-timescale QPOs beating with the spin period of the white dwarf. We determine the spectral class of the companion to be consistent with its quiescent classification and find no significant evidence for irradiation over its inner face. We detect the white dwarf spin period in line fluxes, V/R ratios and Doppler-broadened emission profiles.

Key words:

accretion, accretion discs – binaries: close – line profiles – stars: cataclysmic variables – stars: individual: GK Per – X-rays: stars.

1 INTRODUCTION

GK Per (Nova Per 1901; Campbell 1903), belongs to a subgroup of cataclysmic variables (CVs) called Intermediate Polars (IPs). In these systems an asynchronously-rotating, magnetic white dwarf accretes material from a less-massive, late-type companion filling its Roche lobe. Gas leaving the companion star attempts to form an accretion disc around the primary star but its magnetic field either prevents the formation of the disc or truncates it near the white dwarf.

GK Per was identified with the X-ray source A0327+43 by King, Ricketts & Warwick (1979) and confirmed as an IP by the detection of a 351 s X-ray spin pulse by Watson, King & Osborne (1985; hereafter WKO) and Norton, Watson & King (1988). The same period was subsequently found in optical photometry by Patterson (1991). GK Per has the longest orbital period from the sample of known CVs, $P_{\text{orb}} = 2$ d, (Crampton, Cowley & Fisher 1986; hereafter CCF). The wide binary separation combined with a relatively weak magnetic field (~ 1 MG) means that a truncated accretion disc must be present if current theories of disc formation are correct (Hameury, King & Lasota 1986). The presence of a disc has yet to be confirmed by direct observation, although the system does undergo dwarf nova outbursts every 2–3 years where its optical brightness increases from 13th to 10th magnitude (Sabbadin & Bianchini 1983). The most-

likely mechanism for dwarf nova outbursts is a thermal instability within an accretion disc (Osaki 1974). GK Per outbursts have been modelled as such by Cannizzo & Kenyon (1986) and Kim, Wheeler & Mineshige (1992).

This paper is a continuation of paper I (Morales-Rueda, Still & Roche 1996), in which we presented spectrophotometric observations of GK Per taken on the rise to its 1996 outburst (Mattei et al. 1996). We reported the detection of quasi-periodic oscillations (QPOs) within the Doppler-broadened emission lines of H I and He II. This provides an opportunity to map the velocity structure of the oscillations. QPOs are defined as low-coherence brightness oscillations thought to be associated with material within the inner accretion flows of CVs. Theoretical models developed to explain QPOs consider the presence of dense blobs of material orbiting in the inner regions of the accretion disc (Bath 1973), or non-radial pulsations over the surface of the white dwarf (Papaloizou & Pringle 1978), or radially-oscillating acoustic waves in the inner disc (Okuda et al. 1992; Godon 1995). In these models, the QPO timescales match observations of dwarf novae and are of the order of a few hundred seconds. However the QPO periods detected in GK Per are an order of magnitude longer than this. Previous to this paper they have only been detected in X-ray data taken during outbursts; WKO discovered them in 1.5–8.5 keV EXOSAT data at the peak of the 1983 outburst, while Ishida

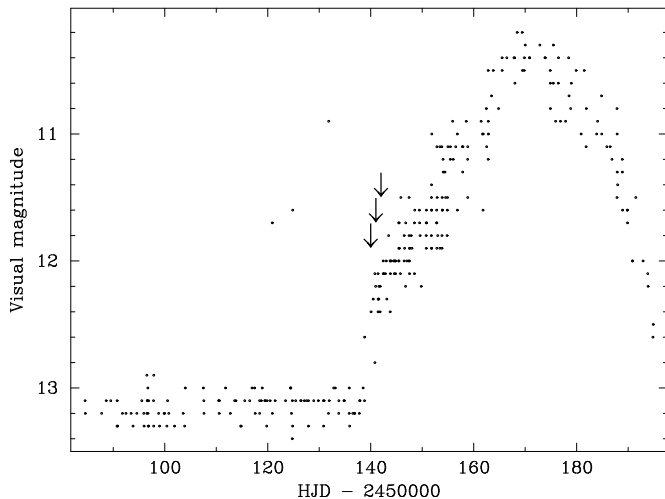


Figure 1. The visual light curve of GK Per during the 1996 outburst obtained from the Variable Star Network (<http://www.kusastro.kyoto-u.ac.jp/vsnet/>). The arrows indicate the times of our spectrophotometric observations.

et al. (1996) report a second detection at 0.7–10 keV with ASCA during the rise to the 1996 outburst discussed in this paper.

To explain the long timescales WKO suggested the QPO mechanism is caused by beating between the 351 s white dwarf spin period and inhomogeneous gas orbiting at the inner edge of the accretion disc. Hellier & Livio (1994; hereafter HL) noted that the X-ray hardness ratio varies over the QPO cycle as expected from photoelectric absorption by cool gas and that a period of a few thousand seconds is consistent with the orbital frequency of gas if it is deposited onto the disc by a gas stream which has partially avoided impacting the outer disc rim and follows a ballistic trajectory. They propose that the QPO mechanism is X-ray absorption by vertically-extended blobs of gas orbiting at this preferred inner impact radius. In paper I we determined that the characteristic velocity structure of the optical counterpart to the QPOs observed by Ishida et al. (1996) is consistent with blobs in the inner disc. In the current paper we present further analysis which indicates that the optical QPO is also driven by absorption, but favours strongly a beat model over the disc-overflow interpretation.

2 OBSERVATIONS

Between 1996 February 26 and 28, 6–8 days before the ASCA pointings of Ishida et al. (1996), we obtained spectrophotometry of GK Per using the Intermediate Dispersion Spectrograph mounted on the 2.5 m Isaac Newton Telescope (INT) on La Palma. Table 1 gives a journal of observations. In Fig. 1 we show a visual light curve obtained by the Variable Star Network during the 1996 outburst, with arrows indicating the days on which we made observations. The quick readout mode was used in conjunction with a Tektronix CCD windowed to 1024×150 pixels to reduce dead

Table 1. Journal of observations. E is the cycle number plus binary phase with respect to the ephemeris given by Crampton, Cowley & Fisher (1986). Phases have been adjusted by $\pi/2$ so that phase 0 corresponds to superior conjunction of the white dwarf.

Date (1996 Feb)	Start (UT)	End (UT)	Start ($E - 2000$)	End ($E - 2000$)	No. of spectra
26	20.06	0.12	617.119	617.204	109
27	20.04	0.07	617.620	617.704	116
28	20.06	0.04	618.121	618.204	117

time and obtain good sampling of the spin cycle. The exposure times and resolution of the data were already described in paper I.

After debiasing and flat-fielding the frames by tungsten lamp exposures, spectral extraction proceeded according to the optimal algorithm of Horne (1986). The data were wavelength calibrated using a CuAr arc lamp and corrected for instrumental response and extinction using the flux standard HZ 15 (Stone 1977). The spectrograph slit orientation of PA 249.1° allowed a 15th magnitude nearby star approximately 0.5 arcsec ENE of GK Per to be employed as calibration for light losses on the slit.

We also have available to us spectroscopy of various K-type stars from 1995 October 11 to 13 obtained from the INT and from 1995 October 30 to November 2 with the 2.1 m telescope in the McDonald Observatory in Texas. The INT instrumental setup was identical to the one used for the 1996 observations described above. For the McDonald data, the low-to-moderate resolution spectrometer ES2 was employed in conjunction with the TII CCD and a grating ruled at $1200 \text{ lines mm}^{-1}$ covering the wavelength region $\lambda 4196 \text{ \AA} - \lambda 4894 \text{ \AA}$ giving a resolution of 200 km s^{-1} at H β .

The spectra were flat-fielded, optimally extracted and wavelength calibrated also in the standard manner. Flux calibrations were applied using observations of the standards HD19445 (Oke & Gunn 1983) and Feige 110 (Stone 1977) for the October and November data respectively. Table 2 gives a list of the K-type templates observed over both runs.

3 RESULTS

3.1 Average spectra

Fig. 2 presents the average of all the data collected on 1996 Feb 28. It is characterised by a flat continuum, broad Balmer and He I lines in emission, high excitation lines of He II, N III and C III and numerous faint, narrow absorption features of Fe I, Ca I, Ti II and Sr II that had been identified as signatures of the K-type secondary star by Kraft (1964), Gallagher & Oinas (1974), CCF and Reinsch (1994).

We employed K star spectral templates to determine which luminosity class best matched the secondary star in this system during outburst and search for signatures of increased X-ray irradiation. Using CCF's fit to the orbital radial velocity of the secondary star we shifted out the orbital motion of the absorption lines with a quadratic rebinning algorithm. We binned in velocity the spectra of GK Per and the K-type templates to ensure that they all had identical wavelength ranges and dispersions. We employed the optimal subtraction algorithm of Marsh, Robinson & Wood

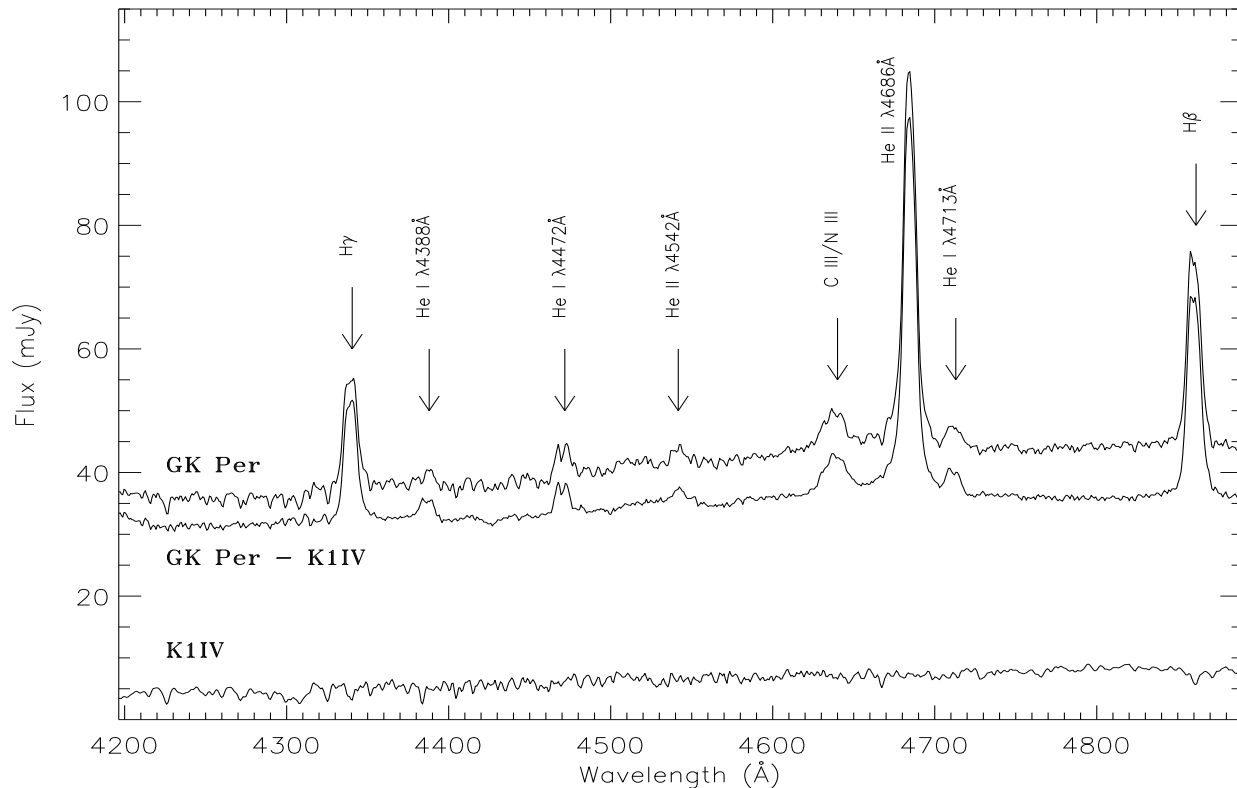


Figure 2. The top spectrum is an average of all GK Per spectra obtained during the third night of observations. The bottom spectrum corresponds to the K1IV template HD197964 multiplied by 3×10^{-4} . The middle spectrum is the residual resulting from the subtraction of the template from the averaged GK Per spectrum and probably resembles the spectrum of the accretion flow.

(1994) to determine the K star spectral type – we multiply the template by a monochromatic constant which represents the contribution to the spectrum from non-stellar sources of light and subtract the resulting spectrum from the GK Per data. The residual was smoothed using a high-pass band filter (FWHM of gaussian = 13 Å), and a χ^2 test performed between the original and smoothed residual. This is an iterative procedure to determine the optimum value of the monochromatic constant which continues until χ^2 is minimised. Table 2 lists the templates, their spectral classes, and the reduced χ^2 obtained after applying optimal subtraction. The best fit template is the K1IV star HD197964 which provided a reduced χ^2 of 2.5. The secondary star contributes 13 per cent of the total light in this spectral region on the third night of observations. This compares to 33 per cent found by CCF and Gallagher & Oinas (1974) during quiescence indicating that the accretion flow has increased in brightness.

The best-fit luminosity classes are consistent with the quiescent classifications of K2IVp by Kraft (1964), K2IVp–K2V by Gallagher & Oinas (1974), K0III by CCF, and K3V by Reinsch (1994). We find the spectral type to be constant across our two phase samples - one during which a large area of the white dwarf-facing surface is visible and the other when it is mostly limb-occulted. Consequently there

Table 2. A list of template K star used to determine the best-fit spectral type for the secondary star.

Name	Spectral type	χ^2	Name	Spectral type	χ^2
October 1995			November 1995		
HR190	K1III	4.3	13 Lac	K0III	4.0
HR8688	K1III	6.6	1 Peg	K1III	5.7
HR8415	K2III	6.5	69 Aql	K2III	3.9
HR8632	K3III	6.2	39 Cyg	K3III	4.0
HR8974	K1IV	5.9	33 Vul	K3.5III	3.8
HR8881	K1V	6.2	3 η Cep	K0IV	5.9
HR222	K2V	3.0	HD197964	K1IV	2.5
HR8832	K3V	3.2			

is no observational evidence for an increase in irradiating flux from the accretion regions over the inner face of the companion star, although we are limited by a small range of spectral templates and poor orbital sampling.

In order to measure integrated emission line fluxes from each of the three nights, we fitted a third order polynomial through wavelength bands relatively free of line features ($\lambda\lambda 4147\text{--}4212\text{\AA}$, $\lambda\lambda 4278\text{--}4306\text{\AA}$, $\lambda\lambda 4560\text{--}4608\text{\AA}$, $\lambda\lambda 4770\text{--}4838\text{\AA}$) and subtracted the fit from the data. Fluxes were measured by summing under each line profile and these

Table 3. Emission line fluxes in units of 10^{-13} erg cm $^{-2}$ s $^{-1}$ from the spectra of GK Per on 1996 Feb 26-28. The minimum and maximum fluxes throughout the night as well as the average nightly flux are provided. The error on the average flux is the standard deviation. Negative fluxes correspond to line absorption.

Line	Flux range	Average flux	Flux range	Average flux	Flux range	Average flux
		26/2/96	27/2/96		28/2/96	
H γ	1.24 – 2.97	2.05 ± 0.34	1.57 – 3.31	2.27 ± 0.30	2.09 – 4.03	3.06 ± 0.37
H β	1.43 – 3.63	2.32 ± 0.40	1.73 – 3.27	2.45 ± 0.35	2.17 – 4.57	3.41 ± 0.46
He I $\lambda 4387.9\text{\AA}$	-0.70 – 0.31	-0.04 ± 0.15	-0.18 – 0.29	0.03 ± 0.08	-0.14 – 0.35	0.11 ± 0.09
He I $\lambda 4437.6\text{\AA}$	-0.83 – 0.36	-0.29 ± 0.18	-0.60 – -0.15	-0.34 ± 0.09	-0.68 – -0.23	-0.44 ± 0.09
He I $\lambda 4471.7\text{\AA}$	-0.47 – 0.72	0.13 ± 0.18	-0.36 – 0.41	0.12 ± 0.14	-0.28 – 0.68	0.25 ± 0.18
He I $\lambda 4713.2\text{\AA}$	-0.70 – 0.52	0.02 ± 0.14	-0.18 – 0.27	0.05 ± 0.08	-0.22 – 0.31	0.02 ± 0.10
He I $\lambda 4921.9\text{\AA}$	-0.06 – 0.93	0.38 ± 0.15	0.18 – 0.58	0.39 ± 0.09	0.26 – 1.03	0.68 ± 0.13
He II $\lambda 4541.7\text{\AA}$	-0.46 – 0.25	-0.06 ± 0.14	-0.30 – 0.30	0.02 ± 0.10	-0.21 – 0.26	0.02 ± 0.11
He II $\lambda 4685.8\text{\AA}$	4.01 – 7.36	5.23 ± 0.77	3.24 – 7.72	5.44 ± 0.78	6.04 – 12.19	8.27 ± 0.94
Bowen blend	0.04 – 1.05	0.50 ± 0.17	0.39 – 1.08	0.65 ± 0.13	0.71 – 1.89	1.06 ± 0.17

Table 4. Power indices α obtained from fitting with a power law function to the integrated flux of each emission line and the continuum over the three nights of observations.

Line	Power index	Line	Power index
H γ	2.3 ± 0.1	H β	2.7 ± 0.1
He I $\lambda 4388\text{\AA}$	1.1 ± 0.4	He I $\lambda 4438\text{\AA}$	2.5 ± 0.8
He I $\lambda 4472\text{\AA}$	2.1 ± 0.7	He I $\lambda 4922\text{\AA}$	3.5 ± 0.5
He II $\lambda 4686\text{\AA}$	3.5 ± 0.1	Bowen blend	2.3 ± 0.2
Continuum	2.41 ± 0.01		

are provided in Table 3. The intensity of the continuum, the lines and the relative intensity of He II $\lambda 4686\text{\AA}$ with respect to the Balmer lines, increases from the first night to the last as the system approaches the outburst maximum. We fit the emission lines during the three nights with a power law function of time $F \sim t^\alpha$, and provide the index α for each line in Table 4.

Power-law fits of the form $f_\nu = \nu^\alpha$ on each consecutive night provide $\alpha = -1.61 \pm 0.03$, -1.43 ± 0.03 and -1.39 ± 0.11 . Continuum slope changes slightly within statistical uncertainties during the observing run, the spectra becoming bluer with time consistent with a rise in temperature through the accretion flow. These indices are inconsistent with an accretion disc emitting as a discrete set of blackbodies (Pringle 1981).

A comparison of the Feb 28 averaged spectrum with the spectra presented by Reinsch (1994) reveals that the Balmer line fluxes are ~ 1.7 times larger than during quiescence and the He II $\lambda 4686\text{\AA}$ feature and the C III/N III $\lambda \lambda 4640\text{--}50\text{\AA}$ Bowen blend are ~ 5.3 times brighter. He I $\lambda 4471.7\text{\AA}$ and He I $\lambda 4921.9\text{\AA}$ are 1.4 and 2.3 times brighter during this outburst stage, respectively. In quiescence the Balmer lines are the brightest emission lines, whereas the strongest line in the current data is He II $\lambda 4686\text{\AA}$. Szkody, Mattei & Mateo (1985) and CCF present spectra of GK Per taken during the 1983 outburst maximum and 20 days after outburst respectively in which this behaviour is also clear.

3.2 Radial velocities

In paper I we provided an analysis of the emission line velocities. To complete the radial velocity analysis we now

consider the absorption lines. In Sec. 3.1 we determined that our best secondary star template has a spectral type of K1IV. By masking out the emission lines in individual GK Per data and subtracting fits to the continua from all spectra, we were able to cross-correlate the absorption spectrum of GK Per with our template (Tonry & Davis 1979). We corrected the resulting radial velocities by the systemic velocity of the template star (-6.5 km s $^{-1}$; Evans 1979) and fitted them with a circular function:

$$V = \gamma + K \sin 2\pi[\phi - \phi_0] \quad (1)$$

Orbital phases were adopted relative to the corrected CCF ephemeris, where ϕ_0 corresponds to superior conjunction of the white dwarf. γ represents the systemic velocity of the binary, K is the radial velocity semiamplitude of the companion star and ϕ is the orbital phase.

We combined the radial velocities measured by previous authors (Kraft 1964; CCF; Reinsch 1994) with our own values and plot them together in Fig. 3. We assume that the errors on all individual measurements previous to this study are equal to the mean error of 20 km s $^{-1}$. The solid curve is the fit to all data, providing $\gamma = 30 \pm 1$ km s $^{-1}$, $K = 119 \pm 2$ km s $^{-1}$ and $\phi_0 = 0.998 \pm 0.003$. The dot-dashed curve is a fit to all the data excluding the current set where $\gamma = 22 \pm 2$ km s $^{-1}$, $K = 128 \pm 2$ km s $^{-1}$ and $\phi_0 = 0.009 \pm 0.003$, providing reasonable agreement although the fits are not consistent within the given errors. Martin (1988) showed that an elliptical fit can account approximately for irradiation processes over the inner face of the secondary star. Elliptical fits to the quiescent data have already been produced by CCF and Reinsch (1994). We do not have suitable phase sampling to produce a significant elliptical fit with the current data. Therefore although we find no evidence for secondary star irradiation in the absorption line radial velocities during outburst, our phase coverage prevents us from ruling it out.

3.3 Emission line profiles

The continuum-subtracted data are presented as time-series of selected line profiles over each night of observation in Fig. 4. At times these lines display double-peaked profiles. This is often considered a signature of accretion disc emis-

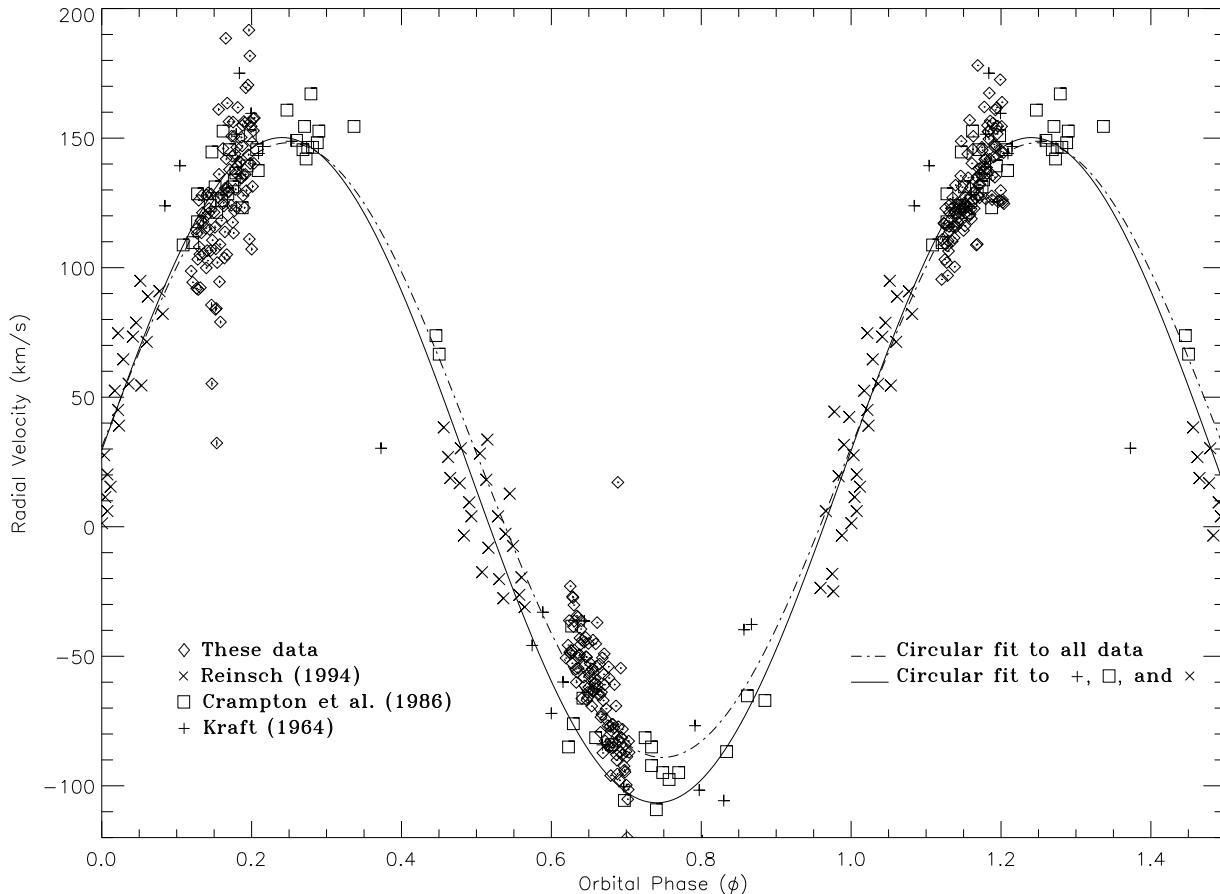


Figure 3. Radial velocities obtained from the current data by cross-correlating absorption features from the companion star against a K1IV template, combined with similar measurements during quiescence from Kraft (1964), CCF, and Reinsch (1994). We provide two circular fits to the data.

sion (Smak 1981), however the velocity structure across the accretion flow is so complex in IPs that this cannot be considered a conclusive detection of the accretion disc. The profiles are asymmetric where the peak apparently shifts from the blue to the red and back again in the Balmer lines over the observations. This behaviour is reminiscent of emission from a localised region in the system such as the bright spot where the accretion stream strikes the outer rim of the disc, or an irradiated region on the secondary star, but we note that the orbital phasing of the observed $H\beta$ feature is inconsistent with both interpretations. Moreover, the orbital phases at which we see these variations are not those at which the hot spot and the irradiated face of the secondary are best observed, i.e. phases 0.8 and 0.5 respectively. The profile variations of the $He\text{I}$ and $He\text{II } \lambda 4686 \text{ \AA}$ lines are different to those of $H\beta$ either because they originate from different locations or are more sensitive to intervening absorption regions.

The most interesting variation occurs in the blue wings of all these profiles. First we note that the profiles are asym-

metric about their rest velocities, regardless of orbital phase, where each line has a red bias. This shift is much larger than the systemic velocity of the binary, measured from secondary star photospheric lines. Secondly we note that this asymmetry is periodic, at least in $H\beta$ and $He\text{II } \lambda 4686 \text{ \AA}$, and this period corresponds to the kilo-second QPOs we reported in paper I. The QPOs manifest in blue-shifted material and appear to be the result of absorption either of the line source or the underlying continuum. We have presented trails of $H\beta$ and $He\text{II } \lambda 4686 \text{ \AA}$ against QPO phase after subtracting the nightly average from each spectrum in paper I.

After the orbital period, the third likely signal present in these trails is the 351 s spin period of the white dwarf. We attempted to remove the orbital variations in the line profile by shifting out the motion of the white dwarf according to the ephemeris and radial velocity fit of CCF. The QPO contribution was accounted for approximately by combining the resulting spectra into 40 bins phased over the QPO cycle and subtracting the spectrum in the bin nearest in time from each individual spectrum. Fig. 5 shows the resulting trails

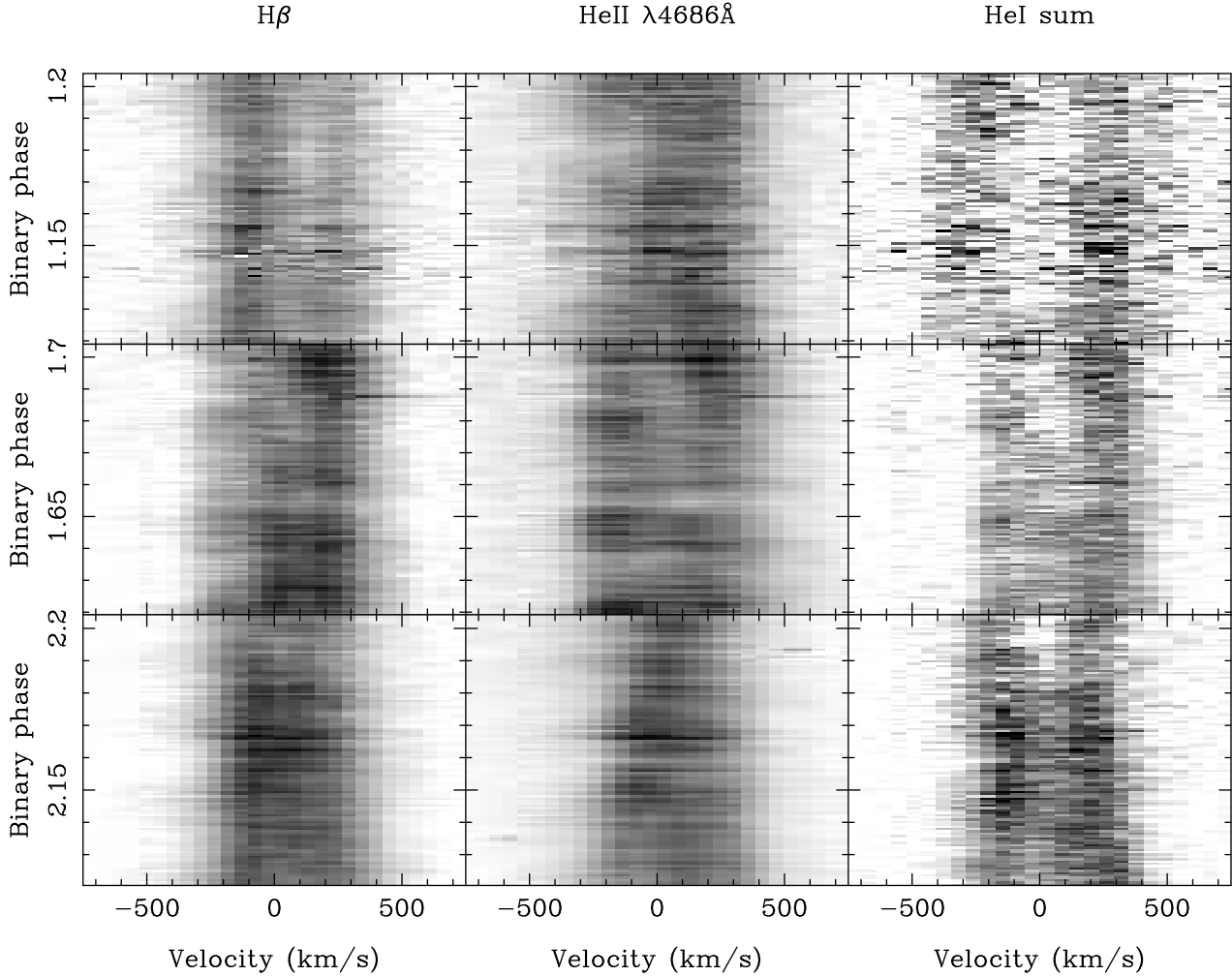


Figure 4. Triled spectra of $H\beta$, $He\ II\ \lambda 4686\ \text{\AA}$ and the average of $He\ I\ \lambda 4388\ \text{\AA}$, $He\ I\ \lambda 4472\ \text{\AA}$, $He\ I\ \lambda 4713\ \text{\AA}$, $He\ I\ \lambda 4922\ \text{\AA}$. Each row corresponds to a different night, the top row being the first night of observations. Images have separated linear greyscales where black corresponds to emission.

of $H\beta$, $He\ II\ \lambda 4686\ \text{\AA}$ and the sum of the He I lines binned into 30 bins, over the spin period using Ishida’s et al. (1992) ephemeris. The modulated signal is faint during the Feb 26 and 27, but clearly present in the $H\beta$ and $He\ II\ \lambda 4686\ \text{\AA}$ profiles on Feb 28 extending out as far as $\sim 1000\ \text{km s}^{-1}$ in the $H\beta$ profile. We see one modulation per cycle with signal moving from the red peak to the blue. This is reminiscent of the spin signal found in the trails of the IP RX J0558+5353 (Still, Duck & Marsh 1998), although in that case most of the power occurred on the 1st harmonic of the spin period, indicating accretion onto two poles of the primary star. In the current trails of GK Per we see no evidence for power on the 1st harmonic. Harlaftis & Horne (1998) postulate that the origin of this spin pulsed emission is the region where the disc material is threaded onto the magnetic field. Similar trails but for spectra obtained during quiescence are presented by Reinsch (1994), where the spin signal is also clear on the fundamental frequency in the Balmer and $He\ II\ \lambda 4686\ \text{\AA}$ lines but not very strong in He I.

3.4 V/R ratios

By measuring the fluxes under the continuum-subtracted blue wings (from -1100 to $0\ \text{km s}^{-1}$) of the $H\beta$ and $He\ II\ \lambda 4686\ \text{\AA}$ lines and dividing these by the flux under the red wings (from 0 to $1100\ \text{km s}^{-1}$) we produce a time-series of V/R ratios. These are plotted in Fig. 6 for the three nights of observation. Kilo-second oscillations are observed over all three nights. A power search over the ratios was performed using the Lomb-Scargle algorithm (Scargle 1982) and the QPO periods found are listed in Table 5. The errors quoted are only an estimate of the minimum error and depend on the frequency sampling. A significance test (a variant of the randomisation Monte Carlo technique, Linnell Nemeč & Nemeč 1985) was run by iteratively searching for periods after small shifts of the data had been performed. After 1000 permutations we found that the periods present in the V/R ratios are within the quoted errors with 95 per cent confidence. Note that the QPOs tend to shorter periods over the three nights.

In order to determine the nature of higher-frequency

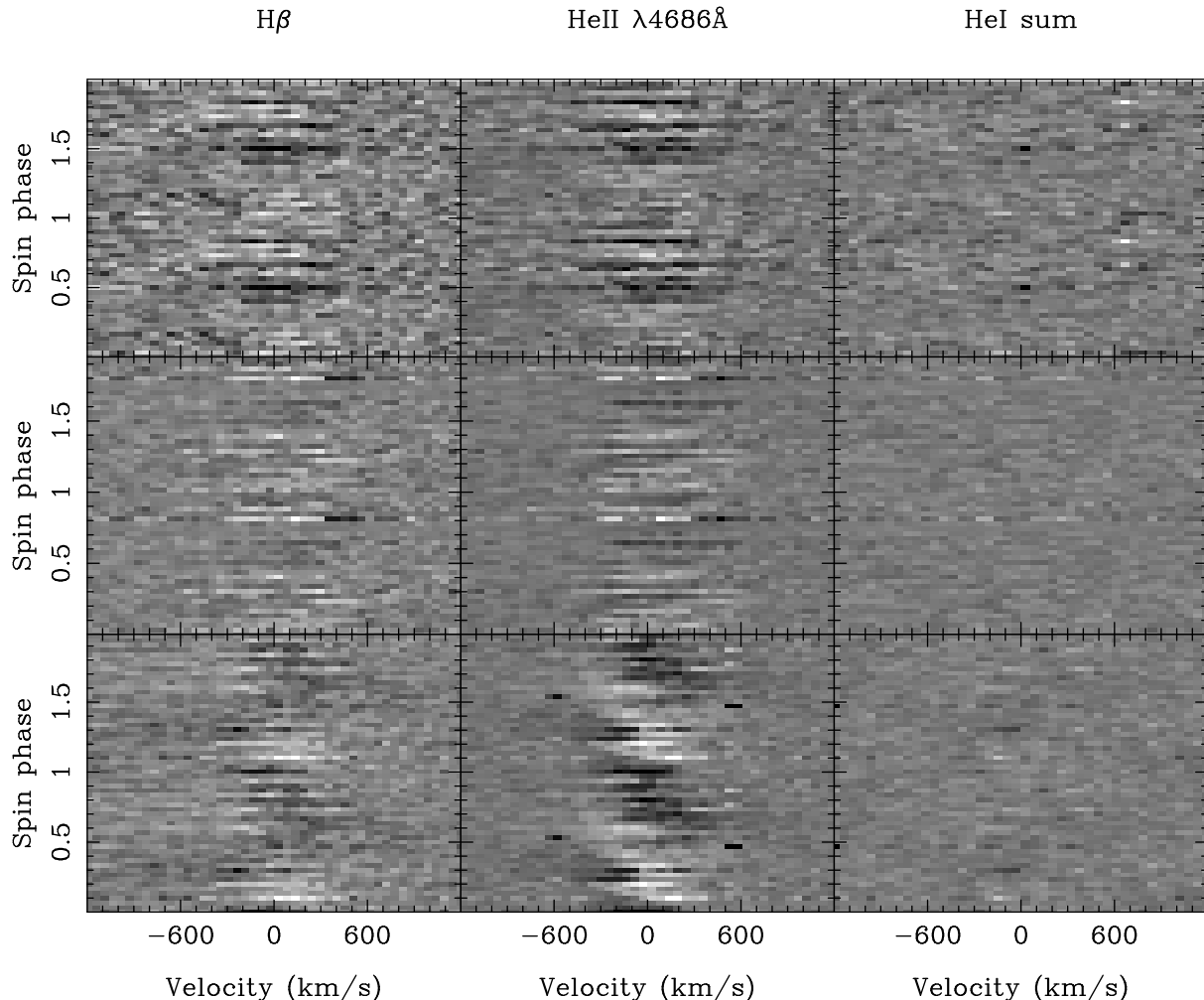


Figure 5. Triled spectra of $H\beta$, $\text{He II } \lambda 4686 \text{ \AA}$ and the average of He I (as in Fig. 3) binned in the spin period. Note that the spin cycle is repeated twice. As in Fig. 3, each row represents a different night, the top row being the first night. Each image is on a separate linear intensity scale.

Table 5. QPO periods measured from the V/R ratios of $H\beta$ and $\text{He II } \lambda 4686 \text{ \AA}$.

1996 Feb	P_{QPO}	1996 Feb	P_{QPO}
$H\beta$ 26th	6362 ± 3	$\text{He II } \lambda 4686 \text{ \AA}$ 26th	6568 ± 3
$H\beta$ 27th	5025 ± 2	$\text{He II } \lambda 4686 \text{ \AA}$ 27th	5241 ± 2
$H\beta$ 28th	3964 ± 1	$\text{He II } \lambda 4686 \text{ \AA}$ 28th	4333 ± 1

variations we created a coarse version of each V/R curve over 40 time bins on each night, each bin approximating to one white dwarf spin cycle. The QPO signal was filtered out by subtracting the bin nearest in time from each V/R measurement. We searched for power in the modified V/R ratios using the Lomb-Scargle algorithm and obtained the power spectra plotted in Fig 7.

Four of the spectra clearly show power at the white dwarf spin period ($246 \text{ cycles day}^{-1}$), but we cannot determine whether there is any power on the 1st harmonic which occurs beyond the Nyquist limit. We folded the modified V/R ratio data using the spin ephemeris from Ishida

et al. (1992) using 40 bins and plot them in Fig. 8. The V/R ratios show sinusoidal behaviour but not as clearly as in Garlick et al. (1994) and Reinsch’s (1994) quiescence data. The maximum in these curves has previously been observed in quiescence at spin phase 0 rather than phase 0.25.

3.5 Emission line and continuum fluxes

We conducted a power search across the same regions of continuum listed in Sec. 3.1 and the integrated flux over each emission line. Power is present at kilo-second periods whose values decrease on consecutive nights; see Table 6 and in Fig. 9 we present the power spectra for the integrated fluxes of $H\beta$, $\text{He II } \lambda 4686 \text{ \AA}$ and the continuum. No significant power was found in the spin period during any of the nights. Garlick et al. (1994) and Reinsch (1994) find clear modulations in the intensity of the Balmer lines with the spin period during quiescence but no significant contributions at the spin period in the continuum.

By means of a power search across radial velocity data,

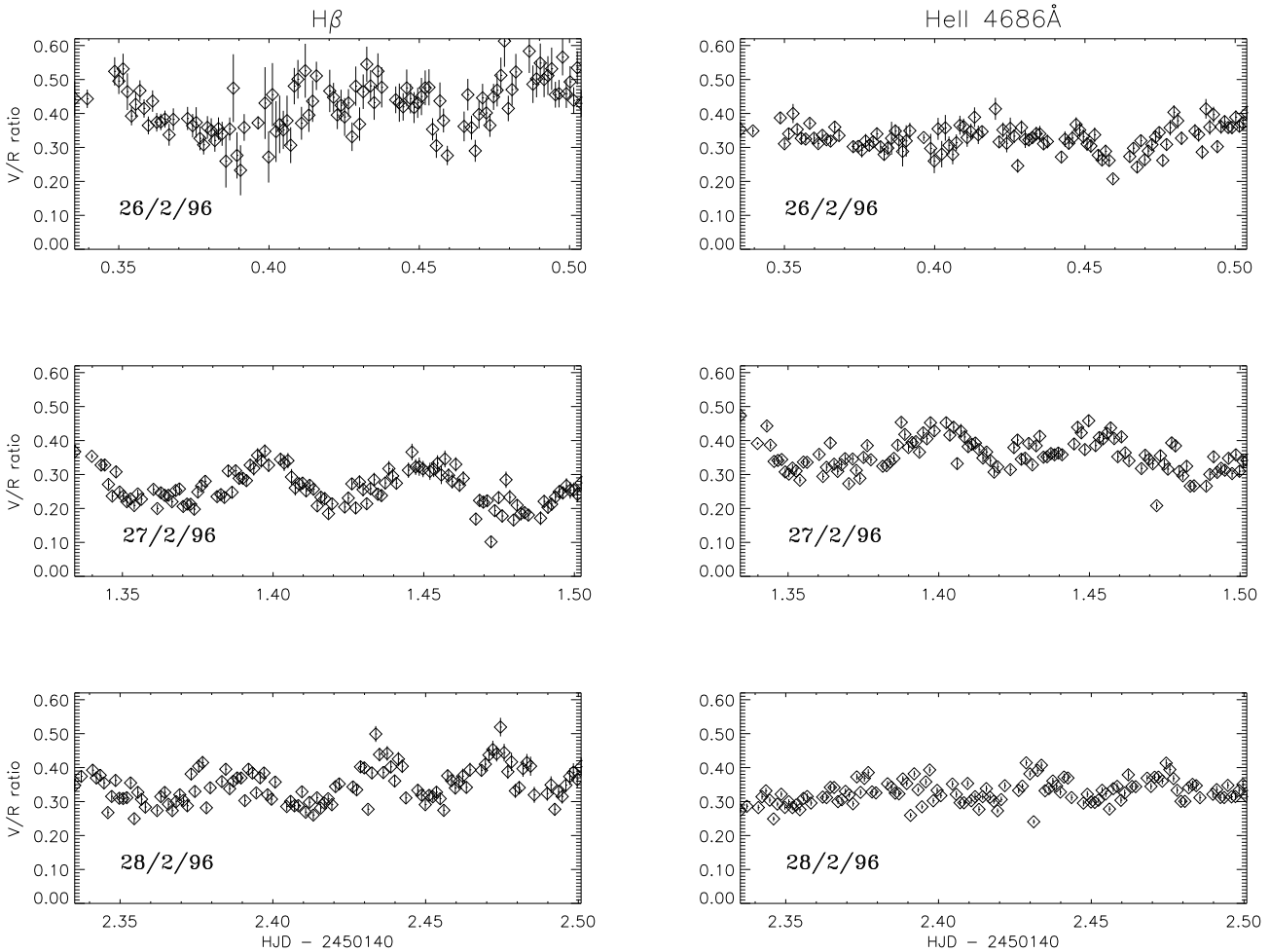


Figure 6. V/R ratio versus HJD for $H\beta$ and $\text{He II } \lambda 4686 \text{ \AA}$. We find QPOs during all three nights.

paper I determined that the characteristic velocities of the QPO signal were intermediate between the orbital regime and the spin regime. This is consistent with a signal origin in the inner disc or the threading region between disc and magnetic curtain. However the search had no means to discriminate between blue- and red-shifted material and therefore could say little more about the QPO mechanism. In this paper we conduct a similar power search but in the line fluxes across discrete velocity bins of the emission profiles. The resulting power maps for $H\beta$ and $\text{He II } \lambda 4686 \text{ \AA}$ are plotted in velocity–frequency space and provided in Fig. 10, and Table 7 lists the QPO period on different nights sampled at -400 km s^{-1} and -600 km s^{-1} in the line profile.

We find that power associated with the QPO is not symmetrically distributed about the rest wavelength, but biased towards the blue wing of each line, as we have previously noted in Sec. 3.3. QPO power extends from -500 to -1000 km s^{-1} depending on the line and night but the QPO does not appear to be a strong function of velocity consistent with our results from paper I. We also find, the QPO tending to longer frequencies with time, as we have already determined from paper I and the V/R ratio analysis in the

current paper. We discuss the significance of this result in Sec. 4.

We also find power on the white dwarf spin frequency extending to $\sim 1000 \text{ km s}^{-1}$, although weaker than we have found in the radial velocity analysis of paper I.

4 DISCUSSION: QPO MECHANISMS

In paper I we found that the optical QPOs observed during the 1996 outburst have a velocity structure that is consistent with a mechanism where dense blobs of gas orbit in the inner disc at a radius determined by the impact of an overflowing gas stream (HL). We determined that the QPO is an approximately constant function of velocity ruling out mechanisms involving radial or vertical oscillations in the inner disc flow (Carroll et al. 1985), and that the QPO tends to higher frequencies with time. In this paper we have shown that the QPO is biased towards blue-shifted material and we discuss this result in terms of the disc-overflow accretion model and the alternative beat model proposed by WKO.

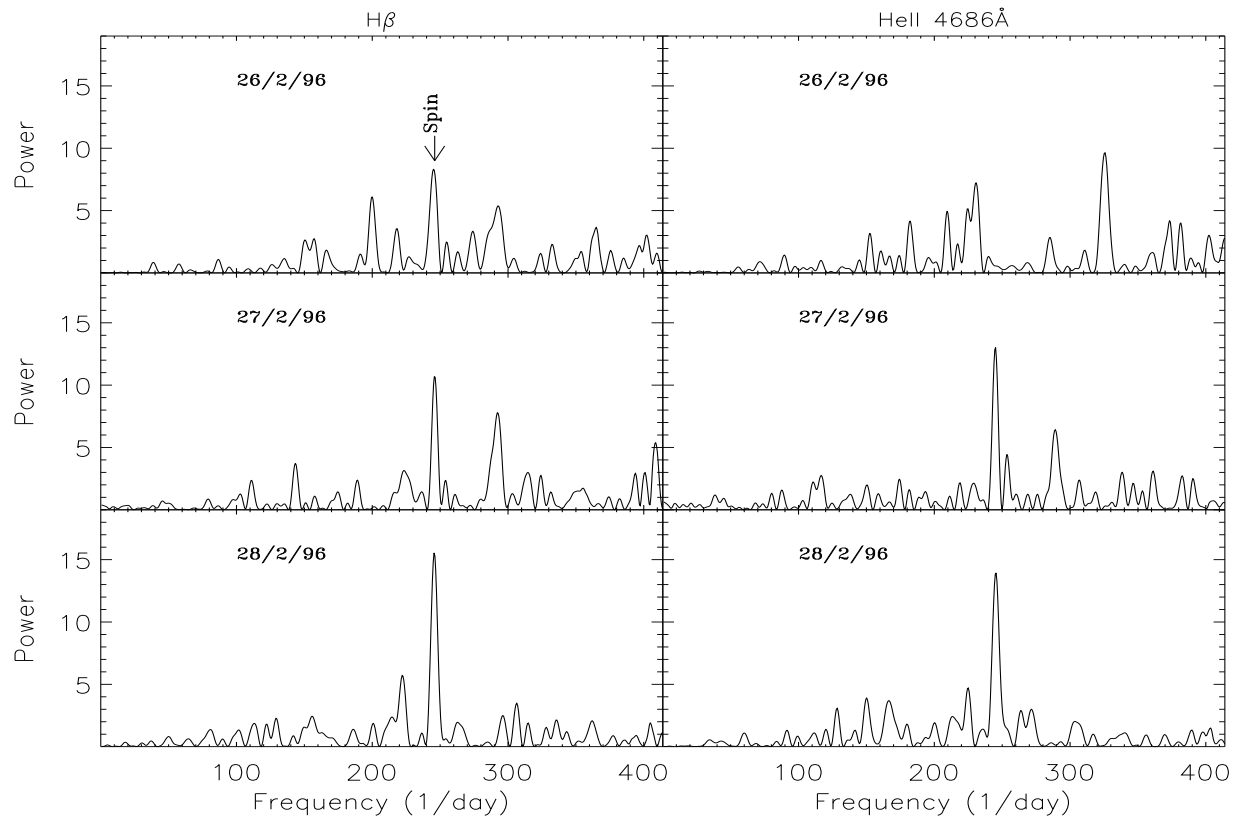


Figure 7. Power spectra obtained from the V/R ratios of H β and He II λ 4686 Å on 1996 Feb 26 to 28 after the QPO has been filtered out.

Table 6. The QPO period determined from the integrated flux of H β and He II λ 4686 Å and for the continuum the three nights of observations. The error given is the minimum error due to the frequency sampling. The third column gives an estimate of the confidence of the identification. This estimate has been obtained by using a randomisation Monte-Carlo Technique over 1000 permutations.

1996 Feb	P_{QPO} (s)	Percentage of Confidence
H β 26th	5932 ± 2	89
H β 27th	4221 ± 1 & 3246 ± 1	95 & 95
H β 28th	3596 ± 1	93
He II 26th	6311 ± 2	90
He II 27th	4435 ± 1 & 3228 ± 1	95 & 95
He II 28th	3447 ± 1	95
Continuum 26th	6750 ± 26	70
Continuum 27th	4477 ± 12	95
Continuum 28th	3692 ± 9	94

4.1 The Disc-overflow accretion model

This model was proposed by HL on the basis that a 5000 s period is consistent with the Keplerian period of blobs of material deposited in the inner disc by the overflowing gas stream (Lubow & Shu 1975; Lubow 1989; Hellier 1993; Armitage & Livio 1996, 1998), and that the X-ray hardness

Table 7. The QPO period determined from bins across the emission line profiles of flux of H β and He II λ 4686 Å on the three nights. Errors are, as in Table 6, the estimates of the minimum error. All periods have been found to be significant to 95 per cent.

1996 Feb	P_{QPO} (s) at -400 km s^{-1}	P_{QPO} (s) at -600 km s^{-1}
H β 26th	6336 ± 2	—
H β 27th	4765 ± 1	4645 ± 1
H β 28th	3766 ± 1	3637 ± 1
He II 26th	6445 ± 2	6378 ± 2
He II 27th	5912 ± 1	—
He II 28th	3725 ± 1	4038 ± 1

ratio measured as a function of QPO phase from the data collected by WKO is consistent with the photo-electric absorption of soft X-rays by cool intervening gas. The optical counterpart to the X-ray QPOs could either be direct reprocessing off the blobs or the periodic reprocessing off material in the outer disc as the blobs intermittently absorb the X-rays from the central object.

We have determined that, in velocity, the QPO ranges between the expected rotational velocity of the outer disc and the overflow impact site (paper 1). Although this distribution of QPO power is consistent with the proposed mechanism, it is more difficult to reconcile the blue-shifted bias of power in terms of the overflow model (Fig. 10).

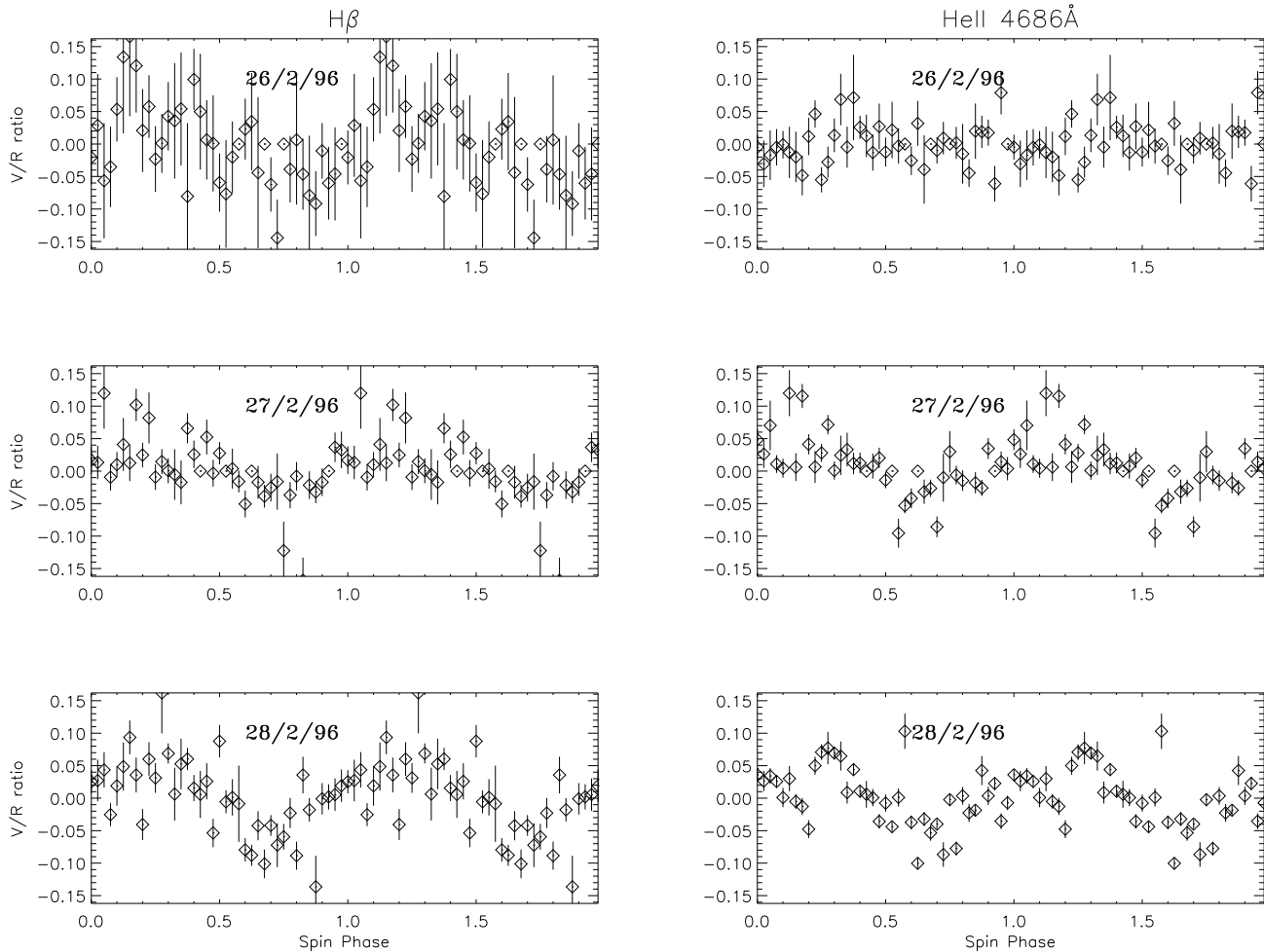


Figure 8. The QPO-filtered V/R ratios versus spin phase obtained for H β and He II $\lambda 4686 \text{ \AA}$ on 1996 Feb 26 to 28. The data are repeated over a second spin cycle.

It is unlikely that the optical QPOs can be the result of reprocessing off the disc unless there is an emission mechanism within the disc which is extremely anisotropic. Similarly direct emission from the blobs must also be anisotropic. In this case the cooling of shocked- or viscous-heating gas within the blobs could cause the anisotropy provided the blobs are orbiting faster than the surrounding disc material. It is not clear why this should be the case.

4.2 A disc-curtain beat mechanism

WKO proposed a QPO mechanism where the observed periods are the beats between the spin frequency of the white dwarf and the Keplerian frequency of dense blobs of gas orbiting at the inner rim of the disc (Alpar & Shaham 1985 a, b). Each time an accretion curtain sweeps over a blob we observe an increase in column density across the curtain, providing a cool absorbing body for the X-ray emission. The prediction follows that the orbital period of the inner disc is either ~ 320 s or ~ 380 s. We investigate whether this model can explain the observed bias in the QPOs across the optical

emission lines. Two schematics of the accretion flow in the binary are depicted in Fig. 11. We take the orbital inclination to be consistent with $46^\circ < i < 72^\circ$ (Reinsch 1994). We have assumed that the magnetic axis of the white dwarf is misaligned with the rotational axis of the system by 45° , although its true inclination is unknown.

In Sec. 3.3 we determined that similar to the X-ray QPOs, the optical counterpart in the emission lines are the result of absorption. We consider two mechanisms which modulate the line emission by absorption over the WKO beat cycle. First we consider self-absorption of line flux from the curtain just above each threading region. Our observation that QPO signal does not extend to as large velocities as the spin signal provides some justification for this assumption. We require the absorption profile to be saturated such that line strength is a function of both column density through the curtain and the velocity gradient across the flow (see e.g. Horne & Marsh 1986). At spin phase equal zero, $\phi_{spin} = 0$ the upper accretion curtain lies behind the white dwarf and material flowing along that curtain is blue-shifted. Conversely material in the curtain feeding the lower pole

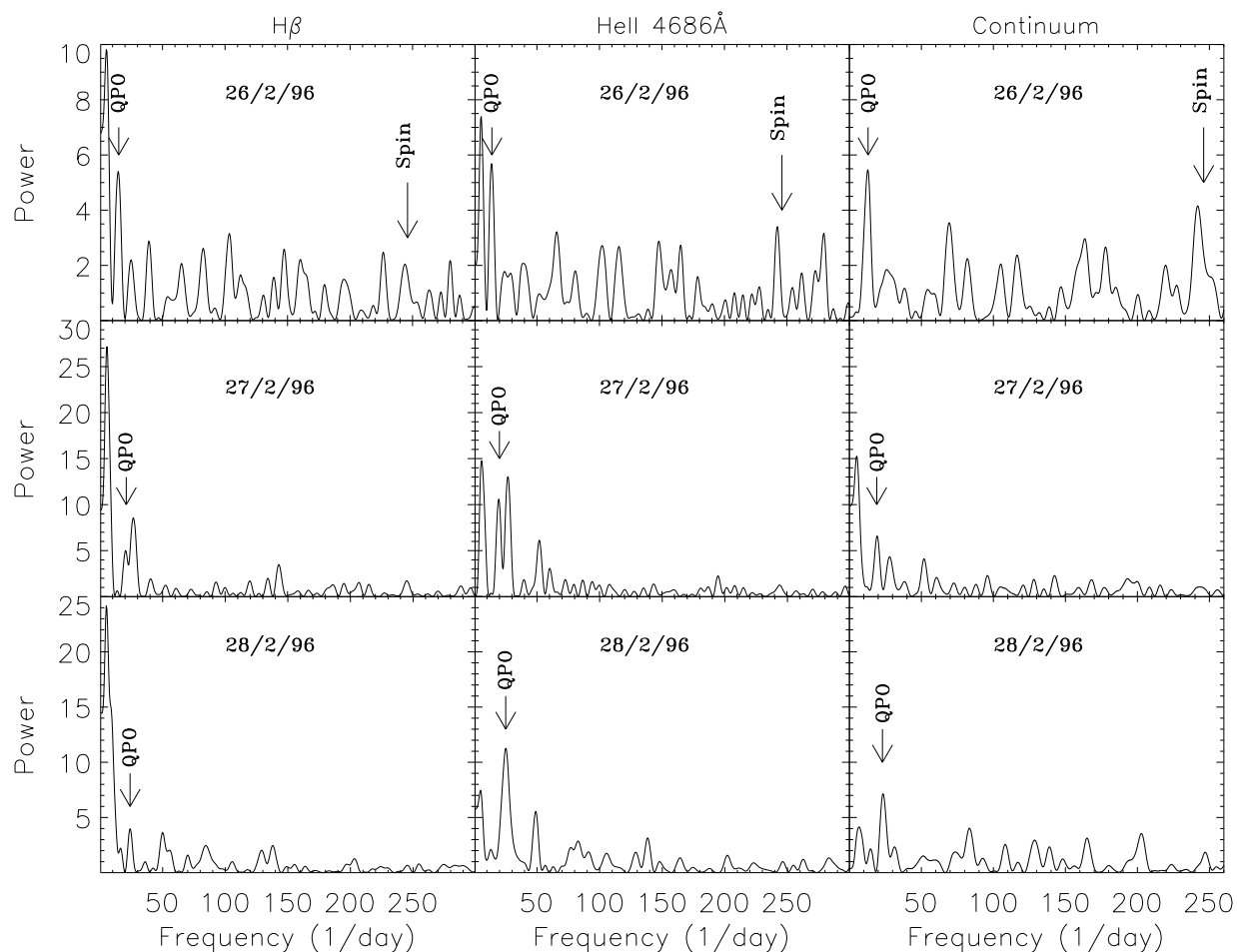


Figure 9. Power spectra for the integrated fluxes of H β , He II λ 4686 Å and the continuum.

is red-shifted. We should observe a blue shifted QPO signal when the blob sweeps through the first threading region every few thousand seconds, increasing the column density along the approaching curtain, but not a red-shifted signal because the second threading region is obscured by the inner accretion disc. The result is a blue bias in the QPO signal across the emission lines at this spin phase. However at $\phi_{spin} = 0.5$ the curtain geometry has rotated by 180° and both curtains are equally visible. But in this configuration the velocity gradient across the line forming regions is small compared to the $\phi_{spin} = 0$ case and consequently the amount of absorption across the line profile is smaller. In this way the blue bias in the signal is conserved over the beat cycle.

An equally plausible alternative is that the absorption is of continuum light from the accretion disc behind the white dwarf. As before, the column density along the accretion curtains is modulated on the beat cycle as a blob sweeps through the threading regions. This provides a kilo-second QPO by periodic absorption which occurs when the upper curtain is back-illuminated by the disc at $\phi_{spin} = 0$. Since there is no back-illuminating source for the lower curtain, or

for the upper curtain when it is red-shifted, this mechanism provides a natural blue bias to the QPO signal.

The beat model explains the long-timescale QPOs from GK Per using the pre-existing models of QPO generation. In these models the driving mechanism has a timescale of a few hundred seconds, as observed in the rest of the dwarf nova class of objects. The extra ingredient for GK Per is provided by its properties as both a dwarf nova and an intermediate polar, where the QPO beats with the accretion curtains which thread the disc onto the rapidly spinning white dwarf to provide the observed kilo-second periods. In the above discussion we have considered the QPO in terms of a blob mechanism but the alternative models of radially-oscillating acoustic waves in the inner accretion disc work equally well. (Okuda et al. 1992; Godon 1995). Consequently we do not require a new physical explanation of QPOs to explain the phenomenon in GK Per.

4.3 QPOs or DNOs?

QPOs are present in dwarf novae during quiescence and outburst. However the kilo-second QPOs in GK Per have to

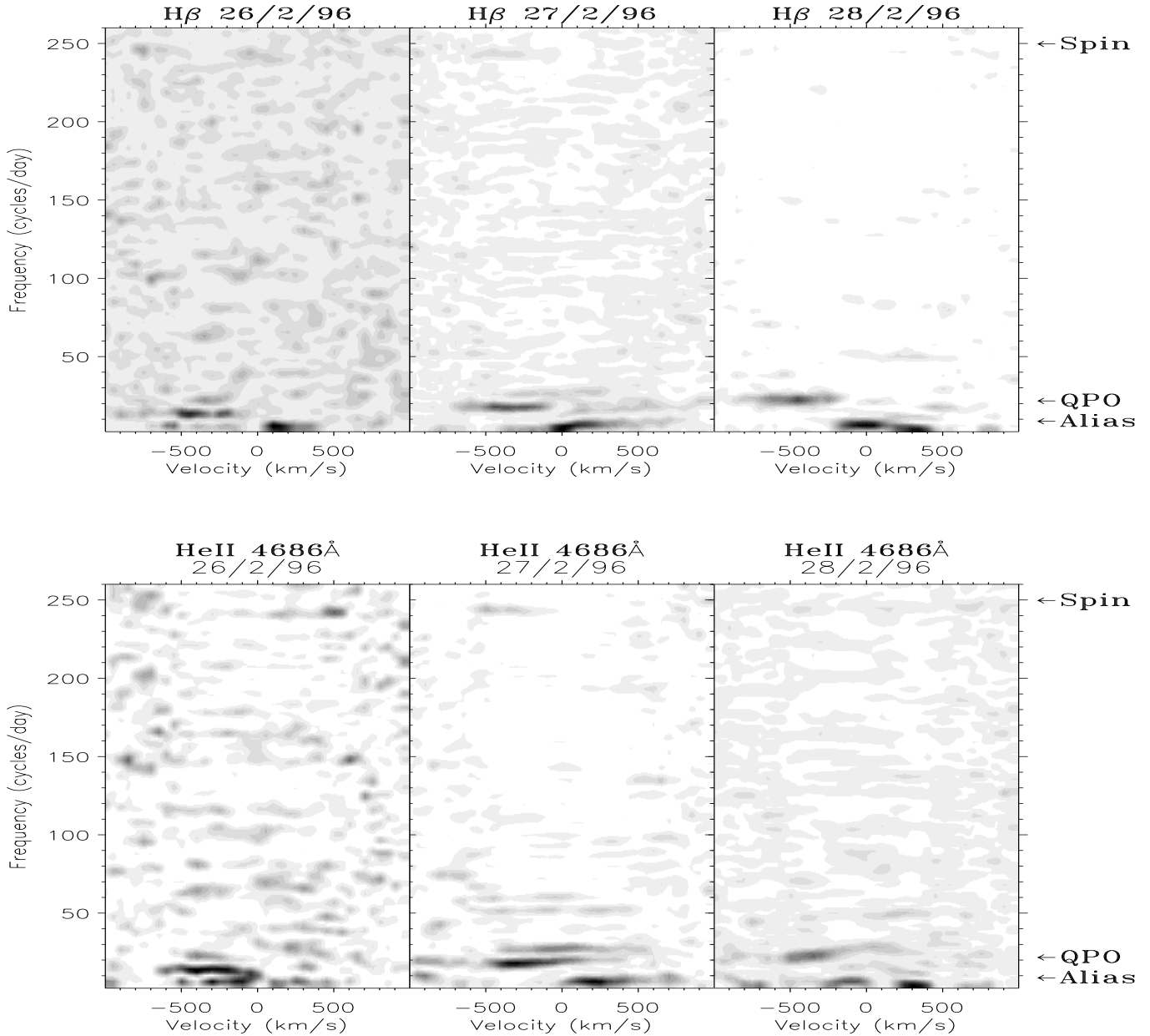


Figure 10. Power maps of frequency versus line velocity obtained from H β and He II $\lambda 4686 \text{ \AA}$ emission line fluxes of GK Per. We detect power at the 4000–6000 s frequency predominantly across the blue wings of these lines. We detect further power at the white dwarf spin frequency (~ 246 cycles/day).

date only been found when the system is in outburst (Reinisch (1994) claims a tentative kilo-second detection in optical photometry but provides no evidence). This behaviour is more typical of another class of oscillations – the dwarf nova oscillations (DNOs), which occur on timescales of tens rather than a few hundred seconds (Robinson and Nather 1979). A characteristic of DNOs is that they tend to shorter periods as a system approaches the peak of its outburst (Patterson 1981), similar to what we have found in the current observations. Given that the beat model is correct, the oscillations found in GK Per show characteristics of both QPOs and

DNOs. The timescales are consistent with QPOs, whereas their behaviour is more comparable to DNOs.

The timescales of DNOs suggest they are driven at the inner edge of an accretion disc (see Warner 1995 for a review in DNOs), and since GK Per is an unusual dwarf nova in that the inner disc is truncated by the white dwarf field, it seems plausible that a DNO mechanism in this system would work on a larger timescale. If we are observing DNOs, the implication of the period increase over the three nights for the beat model is that the inner disc must be orbiting at 320 s rather than 380 s. In the latter case a decrease in the

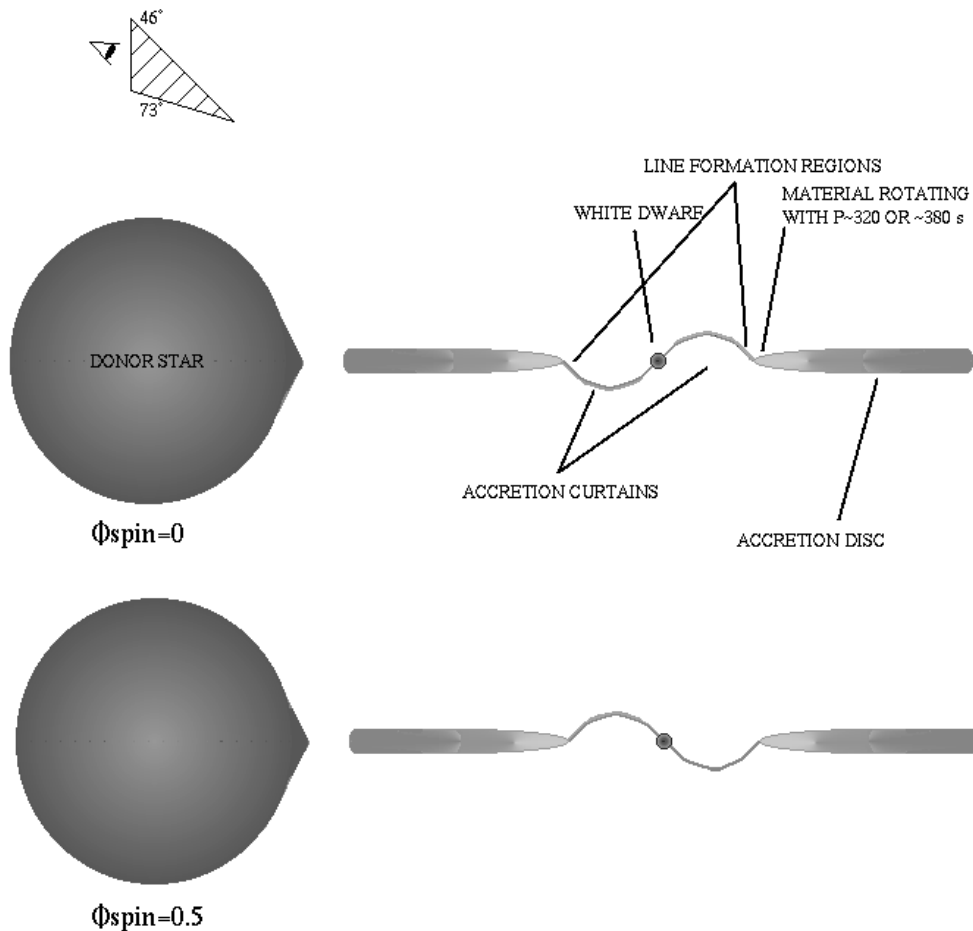


Figure 11. Schematics of the accretion flow in the intermediate polar GK Per. The position of the observer corresponds to orbital phase zero. The two diagrams are slices through a vertical plane across the binary line of centres, separated in time by half a spin cycle.

period of the driving DNO from the disc will result in an increase in the observed beat period. We do not find modulations in our data with either a 320 s or 380 s period. Tentative detections of signal at 390 ± 20 s and 410 ± 13 s have been claimed by Mazeh et al. (1985) from optical photometry during the 1983 outburst while Patterson (1981) reports a detection at 380 ± 20 s but never presented the result. If present during the quiescent state, a 380 s oscillation would suggest a QPOs classification. There have been no reports of a 320 s period in the literature.

5 CONCLUSIONS

We obtain new values for the systemic velocity and the velocity semi-amplitude of the secondary in agreement with previous authors. We conclude that there is no evidence for increased heating over the inner face of the donor star during this stage of the outburst. We find spin modulations in the V/R ratios of the lines but only tentatively in their integrated fluxes or the continuum. Spin power resolved across the line profiles extends to velocities of 1000 km s^{-1} , a large fraction of the freefall velocity of the central object.

The detection of kilo-second QPOs across the optical

emission line profiles of GK Per have provided an opportunity to test the mechanism behind the unique long-timescale QPOs in this object, which are an order of magnitude longer than QPOs normally observed in disc-accreting cataclysmic variables. We have rejected the model of HL which considers the direct effects of blobs orbiting at the Keplerian frequency of the annulus associated with a disc-overflow impact site. Our favoured models consider the long QPO period to be the consequence of beating between more typical timescale QPOs or DNOs of $\sim 300\text{--}400$ s with the magnetic accretion curtain spinning with the white dwarf. Therefore we do not require a new model to explain these long timescales – the long oscillations are merely a consequence of the magnetic nature of the binary.

ACKNOWLEDGEMENTS

We thank Janet Wood and John Lockley for obtaining the spectra of the K-type templates at the McDonald Observatory. MDS was supported by PPARC grant K46019. PDR acknowledges the support of the Nuffield Foundation via a grant to newly qualified lectures in science to assist collaborative research. The reduction and analysis of the data were

carried out on the Sussex node of the STARLINK network. We thank Tom Marsh for providing his reduction software. LM also wishes to thank R. I. Hynes for useful discussion. The Isaac Newton Telescope is operated on the island of La Palma by the Isaac Newton Group in the Spanish Observatorio del Roque de los Muchachos of the Instituto de Astrofísica de Canarias.

REFERENCES

- Alpar, M. A., Shaham, J., 1985a, IAU Circ. No. 4046
 Alpar, M. A., Shaham, J., 1985b, *Nat*, 316, 239
 Armitage, P. J., Livio, M., 1996, *ApJ*, 470, 1024
 Armitage, P. J., Livio, M., 1998, *ApJ*, 439, 898
 Bath, G. T., 1973, *Nature Phys. Sci.*, 246, 84
 Campbell L., 1903, *Harv. Ann.*, 48, 90
 Cannizzo J. K., Kenyon S. J., 1986, *ApJ*, 309, L43
 Carroll, B. W., Cabot, W., McDermott, P. N., Savedoff, M. P., Van Horn, H. M., 1985, *ApJ*, 296, 529
 Crampton D., Cowley A. P., Fisher W. A., 1986, *ApJ*, 300, 788
 Evans, D. S., 1979, *IAU Symp.*, 30, 57
 Gallagher, J. S., Oinas, V., 1974, *PASP*, 86, 952
 Garlick, M. A., Mitaz, J. P. D., Rosen, S. R., Mason, K. O., 1994, *MNRAS*, 269, 517
 Godon, P., 1995, *MNRAS*, 274, 61
 Hameury, J. M., King, A. R., Lasota, J. P., 1986, *MNRAS*, 218, 695
 Harlaftis, Horne, K., 1998, in preparation
 Hellier, C., 1993, *MNRAS*, 265, L35
 Hellier, C., Livio, M., 1994, *ApJ*, 424, L57
 Horne, K., 1986, *PASP*, 98, 609
 Horne, K., Marsh, T. R., 1986, *MNRAS*, 218, 761
 Ishida, M., Sakao, T., Makishima, K., Ohashi, T., Watson, M. G., Norton, A. J., Kawada, M., Koyama, K., 1992, *MNRAS*, 254, 647
 Ishida, M., Yamashita, A., Ozawa, H., Nagase, F., Inoue, H., 1996, *IAU Circ.* 6340
 Kim, S. W., Wheeler, J. C., Mineshige, S., 1992, *ApJ*, 384, 269
 King A. R., Ricketts M. J., Warwick R. S., 1979, *MNRAS*, 187, 77p
 Kraft, R. P., 1964, *ApJ*, 139, 457
 Linnell Nemeč A. F., Nemeč J. M., 1985, *AJ.*, 90(11), 2317
 Lubow, S. H., 1989, *ApJ*, 340, 1072
 Lubow, S. H., Shu, F. H., 1976, *ApJ*, 207, L53
 Marsh, T. R., Robinson, E. L., Wood, J. H., 1994, *MNRAS*, 266, 137
 Martin. J. S., 1988, D. Phil. thesis, University of Sussex
 Mattei, J. A., Bortle, J., Dillon, W., Royer, R., Schmeer, P., Komorous, R. A., Osorio, J. R., McKenna, J., 1996, *IAU Circ.* 6325
 Mazeh, T., Tal, Y., Shaviv, G., Bruch, A., Budell, R., 1985, *A&A*, 149, 470
 Morales-Rueda L., Still M. D., Roche P., 1996, *MNRAS*, 283, L58
 Norton A. J., Watson M. G., King A. R., 1988, *MNRAS*, 231, 783
 Oke, J. B., Gunn, J. E., 1983, *ApJ*, 266, 713
 Okuda T., Kazushige O., Makoto T., Mineshige S., 1992, *MNRAS*, 254, 427
 Osaki, Y., 1974, *PASJ*, 26, 429
 Papaloizou, J., Pringle, J. E., 1978, *MNRAS*, 182, 423
 Patterson, J., 1981, *ApJS*, 45, 517
 Patterson, J., 1991, *PASP*, 103, 1149
 Pringle, J. E., 1981, *ARA&A*, 19, 137
 Reinsch, K., 1994, *A&A*, 281, 108
 Robinson, E. L., Nather, R. E., 1979, *ApJS*, 39, 461
 Sabbadin F., Bianchini A., 1983, *A&AS*, 54, 393
 Scargle, J. D., 1982, *ApJ*, 263, 835
 Smak, J., 1981, *AcA*, 31, 395
 Still, M. D., Duck, S. R., Marsh, T. R., 1998, in preparation
 Stone, R. P. S., 1977, *ApJ*, 218, 767
 Szkody P., Mattei J. A., Mateo M., 1985, *PASP*, 97, 264
 Tonry, J., Davis, M., 1979, *AJ*, 84, 1511
 Watson, M. G., King, A. R., Osborne, J., 1985, *MNRAS*, 212, 917
 Warner, B., 1995, *Cataclysmic Variable Stars*, Cambridge Astrophysics Series, 28, Cambridge Univ. Press